Network Analysis Prioritizes DEWAX and ICE1 as the Candidate Genes for Major eQTL Hotspots in Seed Germination of Arabidopsis thaliana

Hartanto, Margi; Joosen, Ronny V.L.; Snoek, Basten L.; Willems, Leo A.J.; Sterken, Mark G. et al

1 **Title: Network Analysis Prioritizes DEWAX and ICE1 as the Candidate Genes for**

2 **Major eQTL Hotspots in Seed Germination of *Arabidopsis thaliana***

3

4 **Author names and affiliations**

5 Margi Hartanto[*], Ronny V. L. Joosen[†], Basten L. Snoek[‡], Leo A. J. Willems[†], Mark G.

6 Sterken[§], Dick de Ridder[*], Henk W. M. Hilhorst[†], Wilco Ligterink[†], Harm Nijveen[*,**]

7 [*]Bioinformatics Group, Wageningen University, NL-6708 PB Wageningen, The Netherlands

8 [†]Laboratory of Plant Physiology, Wageningen University, NL-6708 PB Wageningen, The

9 Netherlands

10 [‡]Theoretical Biology and Bioinformatics, Utrecht University, 3584 CH Utrecht, The

11 Netherlands

12 [§]Laboratory of Nematology, Wageningen University, NL-6708 PB Wageningen, The

13 Netherlands

14

15

16 **Data availability**

17 Cel files of microarray data have been deposited in the ArrayExpress database at EMBL-EBI

18 (www.ebi.ac.uk/arrayexpress) under accession number E-MTAB-9080. The code for the

19 analysis and visualization is available in the form of R scripts at the Wageningen University

20 GitLab repository (https://git.wur.nl/harta003/seed-germination-qtl).

21

22

23

24

Corresponding authors:

Margi Hartanto, Droevendaalsesteeg 1 6708PB WAGENINGEN, phone number: +31630634476, email: margi.hartanto@wur.nl;

Harm Nijveen, Droevendaalsesteeg 1 6708PB WAGENINGEN, phone number: +31317484706 , email: harm.nijveen@wur.nl

Abstract

Seed germination is characterized by a constant change of gene expression across different time points. These changes are related to specific processes, which eventually determine the onset of seed germination. To get a better understanding on the regulation of gene expression during seed germination, we performed a quantitative trait locus mapping of gene expression (eQTL) at four important seed germination stages (primary dormant, after-ripened, six-hour after imbibition, and radicle protrusion stage) using *Arabidopsis thaliana* Bay x Sha recombinant inbred lines (RILs). The mapping displayed the distinctness of the eQTL landscape for each stage. We found several eQTL hotspots across stages associated with the regulation of expression of a large number of genes. Interestingly, an eQTL hotspot on chromosome five collocates with hotspots for phenotypic and metabolic QTLs in the same population. Finally, we constructed a gene co-expression network to prioritize the regulatory genes for two major eQTL hotspots. The network analysis prioritizes transcription factors DEWAX and ICE1 as the most likely regulatory genes for the hotspot. Together, we have

revealed that the genetic regulation of gene expression is dynamic along the course of seed germination.

INTRODUCTION

Seed germination involves a series of events starting with the transition of *quiescent* to physiologically active seeds and ends with the emergence of the embryo from its surrounding tissues. Germination is initiated when seeds become imbibed by water, leading to the activation of seed physiological activities (Bewley et al. 2013b; Nonogaki et al. 2010). Major metabolic activities occur after seeds become hydrated, for example, restoration of structural integrity, mitochondrial repair, initiation of respiration, and DNA repair (Bewley et al. 2013b; Nonogaki et al. 2010). For some species such as *Arabidopsis thaliana*, germination can be blocked by seed dormancy. Dormant seeds need to sense and respond to environmental cues to break their dormancy and complete germination. In *Arabidopsis thaliana*, seed dormancy can be alleviated by periods of dry after-ripening or moist chilling (Bewley et al. 2013b). Soon after dormancy is broken, the storage reserves are broken down, and germination-associated proteins are synthesized. Lastly, further water uptake followed by cell expansion leads to radicle protrusion through endosperm and seed coat, which marks the end of germination (Bewley et al. 2013b).

A major determinant for the completion of seed germination is the transcription and translation of mRNAs. The activity of mRNA transcription is low in dry, mature seeds (Comai and Harada 1990; Leubner-Metzger 2005), and drastically increases after seeds become rehydrated (Bewley et al. 2013a). Nevertheless, stored mRNAs of more than 12,000 genes with various functions are already present in dry seeds. These mRNAs are not only remnants from the seed developmental process, but also mRNAs for genes related to metabolism as well as protein synthesis and degradation required in early seed germination (Nakabayashi et al. 2005; Rajjou et al. 2004). Later in after-ripened seeds, only a slight

change in transcript composition was detected compared to the dry seeds (Finch-Savage et al.

2007). The major shift in transcriptome takes place after water imbibition (Nakabayashi et al.

2005). Interestingly, the transcriptome at the imbibition stage depends on the status of

dormancy. For non-dormant seeds, most of the transcripts are associated with protein

synthesis, while for dormant seeds, the transcripts are dominated by genes associated with

stress-responses (Finch-Savage et al. 2007; Buijs et al. 2019). Even the transcript composition

in primary dormant seeds, which occurs when the dormancy is initiated during development,

is different from that of secondary dormant seeds, which occurs when the dormancy is

reinduced (Cadman et al. 2006). These findings show the occurrence of phase transitions in

transcript composition along the course from dormant to germinated seed.

As omics technology becomes more widely available, several transcriptomics studies in seed

germination processes have been conducted on a larger-scale. More developmental stages,

i.e., stratification and seedling stage, and even spatial analyses have been included in these

studies, resulting in the identification of gene co-expression patterns as well as the predicted

functions of hub-genes (Narsai et al. 2011; Silva et al. 2016; Dekkers et al. 2013; Bassel et al.

2011). Through guilt-by-association, these co-expression based studies can be used for the

identification of regulatory genes that are involved in controlling the expression of

downstream genes. These regulatory genes can be subjected to further studies by reverse

genetics to provide more insight into the molecular mechanisms of gene expression in seed

germination (i.e., Silva et al. 2016). Nevertheless, this approach still has limitations. Uygun et

al. (2016) argued that co-expressed genes do not always have similar biological functions. On

the other hand, genes involved in the same function are not always co-expressed since gene

expression regulation could be the result of post-transcriptional or other layers of regulation

(Lelli et al. 2012). Further, Uygun et al. (2016) emphasized the importance of combining the

expression data with multiple relevant datasets to maximize the effort in the prioritization of candidate regulatory genes.

Genetical genomics is a promising approach to study the regulation of gene expression by combining genome-wide expression data with genotypic data of a segregating population (Jansen and Nap 2001). To enable this strategy, the location of markers associated with variation in gene expression is mapped on the genome, which results in the identification of expression quantitative trait loci (eQTLs). Relative to the location of the associated gene, the eQTL can be locally or distantly mapped, known as local and distant eQTLs (Rockman and Kruglyak 2006; Brem et al. 2002). Local eQTLs mostly arise because of variations in the corresponding gene or a cis-regulatory element. In contrast, distant eQTLs typically occur due to polymorphism on trans-regulatory elements located far away from the target genes (Rockman and Kruglyak 2006). Therefore, given the positional information of distant eQTLs, one can identify the possible regulators of gene expression. However, the eQTL interval typically spans a large area of the genome and harbors hundreds of candidate regulatory genes. A large number of candidate genes would cause the experimental validation (e.g. using knockout or overexpression lines) to be costly and take a long time. Therefore, a prioritization method is needed to narrow down the list of candidate genes underlying eQTLs, particularly on distant eQTL hotspots. A distant eQTL hotspot is a genomic locus where a large number of distant eQTLs are collocated (Breitling et al. 2008). The common assumption is that the hotspot arises due to one or more polymorphic master regulatory genes affecting the expression of multiple target genes (Breitling et al. 2008). Therefore, the identification of master regulatory genes becomes the center of most genetical genomics studies as the findings might improve our understanding of the regulation of gene expression (i.e., in Keurentjes et al. 2007; Jimenez-Gomez et al. 2010; Sterken et al. 2017; Valba et al. 2015; Terpstra et al. 2010).

In this study, we carried out eQTL mapping to reveal loci controlling gene expression in seed germination. To capture whole transcriptome changes during seed germination, we included four important seed germination stages, which are primary dormant seeds (PD), after-ripened seeds (AR), six-hours imbibed seeds (IM), and seeds with radicle protrusion (RP). In total, 160 recombinant inbred lines (RILs) from a cross between genetically distant ecotypes Bay-0 and Shahdara (Bay x Sha) were used in this study (Loudet et al. 2002). Our results show that each seed germination stage has a unique eQTL landscape, confirming the stage-specificity of gene regulation, particularly for distant regulation. Based on network analysis, we identify the transcription factors ICE1 and DEWAX as prioritized candidate regulatory genes for two major eQTL hotspots in PD and RP, respectively. Finally, the resulting dataset complements the previous phenotypic QTL (Joosen et al. 2012) and metabolite QTL (Joosen et al. 2013) datasets, allowing systems genetics studies in seed germination. The identified eQTLs are available through the web-based AraQTL (http://www.bioinformatics.nl/AraQTL/) workbench (Nijveen et al. 2017).

MATERIALS AND METHODS

Plant materials

In this study, we used 164 recombinant inbred lines (RILs) derived from a cross between the Bay-0 and Shahdara Arabidopsis ecotypes (Loudet et al. 2002) provided by the Versailles Biological Resource Centre for Arabidopsis (http://dbsgap.versailles.inra.fr/vnat). The plants were sown in a fully randomized setup on 4x4 cm rockwool plugs (MM40/40, Groudan B. V.) and hydrated with 1 g/l Hyponex (NPK = 7:6:19, http://www.hyponex.co.jp) in a climate chamber (20°C day, 18°C night) with 16 hours of light (35 W/m2) at 70% relative humidity. Seeds from four to seven plants per RIL were bulk harvested for the experiment (see also

148   Joosen et al. 2012; Joosen et al. 2013). The genotypic data consisting of 1,059 markers per

149   line was obtained from Serin et al. (2017). However, the genotypic data is available only for

150   160 RILs; therefore, we used this number of lines for eQTL mapping.

151

152   **Experimental setup**

153   The RIL population was grouped into four subpopulations, each one representing one of the

154   four different seed germination stages. We used the designGG-package (Li et al. 2009) in R

155   (version 3.6.0 Windows x64) to aid the grouping so that the distribution of Bay-0 and Sha

156   alleles between sub-populations is optimized. The first stage is the primary dormant (PD)

157   stage when the seeds were harvested and stored at -80°C after one week at ambient

158   conditions. The second stage is after-ripened (AR) seeds that obtained maximum germination

159   potential after five days of imbibition by storing at room temperature and ambient relative

160   humidity. The third stage is the 6 hours imbibition (IM) stage. For this stage, the seeds were

161   after-ripened and imbibed for six hours on water-saturated filter paper at 20°C and

162   immediately transferred to a dry filter paper for 1 minute to remove the excess of water. The

163   fourth stage is the radicle protrusion (RP) stage. To select seeds at this stage, we used a

164   binocular to observe the presence of a protruded radicle tip.

165

166   **RNA isolation**

167   Total RNA was extracted according to the hot borate protocol modified from Wan and

168   Wilkins (1994). For each treatment, 20 mg of seeds were homogenized and mixed with 800 µl

169   of extraction buffer (0.2M Na boratedecahydrate (Borax), 30 mM EGTA, 1% SDS, 1% Na

170   deoxycholate (Na-DOC)) containing 1.6 mg DTT and 48 mg PVP40 which had been heated

171   to 80°C. Then, 1 mg proteinase K was added to this suspension and incubated for 15 min at

172   42°C. After adding 64 µl of 2 M KCL, the samples were incubated on ice for 30 min and

173   subsequently centrifuged for 20 min at 12,000 g. Ice-cold 8 M LiCl was added to the

174   supernatant in a final concentration of 2 M, and the tubes were incubated overnight on ice.

175   After centrifugation for 20 min at 12,000 g at 4°C, the pellets were washed with 750 μl ice-

176   cold 2 M LiCl. The samples were centrifuged for another 10 min at 10,000 g at 4°C, and the

177   pellets were re-suspended in 100 μl DEPC treated water. The samples were phenol-

178   chloroform extracted, DNAse treated (RQ1 DNase, Promega), and further purified with

179   RNeasy spin columns (Qiagen) following the manufacturer's instructions. The RNA quality

180   and concentration were assessed by agarose gel electrophoresis and UV spectrophotometry.

181

182   **Microarray analysis**

183   RNA was processed for use on Affymetrix Arabidopsis SNPtile array (atSNPtilx520433), as

184   described by the manufacturer. Briefly, 1 mg of total RNA was reverse transcribed using a

185   T7-Oligo(dT) Promoter Primer in the first-strand cDNA synthesis reaction. Following RNase

186   H-mediated second-strand cDNA synthesis, the double-stranded cDNA was purified and

187   served as a template in the subsequent in vitro transcription reaction. The reaction was carried

188   out in the presence of T7 RNA polymerase and a biotinylated nucleotide

189   analog/ribonucleotide mix for complementary RNA (cRNA) amplification and biotin

190   labeling. The biotinylated cRNA targets were then cleaned up, fragmented, and hybridized to

191   the SNPtile array. The hybridization data were extracted using a custom R script with the help

192   of an annotation-file based on TAIR10. Intensity data were log-transformed and normalized

193   using the *normalizeBetweenArrays* function with the quantile method from Bioconductor

194   package limma (Ritchie et al. 2015). Then, for each annotated gene, the log-intensities of anti-

195   sense exon probes were averaged.

196

197   **Clustering analysis**

Principal component analysis for log-intensities of all parents and RIL population samples was done using the pr.comp function in R where the unscaled log intensities are shifted to be zero centered. For hierarchical clustering, we only selected genes with a minimal fold change of 2 between any pair of consecutive stages (PD to AR, AR to IM, or IM to RP). Then, the distance matrices of filtered genes and all samples were calculated using the absolute Pearson correlation. These matrices were clustered using Ward's method. We manually set the number of clusters to 8 and performed gene ontology enrichment for each of the clusters using the weight algorithm of the topGO package in R and used 29,913 genes detected by hybridization probes as the background (Alexa et al. 2006).

eQTL mapping

For eQTL mapping, we used 160 RILs separated into four subpopulations, each representing one specific seed germination stage. For each stage separately, eQTLs were mapped using a single-marker model, as in Sterken et al. (2017). The gene expression data were fitted to the linear model

$$y_{i,j} \sim x_j + e_j$$

where y is the log-intensity representing the expression of a gene i (i = 1, 2, ..., 29,913) of RIL j (j = 1, 2, ..., 160) explained by the parental allele on marker location x (x = 1, 2, ..., 1,059). The random error in the model is represented by e_j.

To account for the multiple-testing burden in this analysis, we determined the genome-wide significant threshold using a permutation approach (e.g. see Sterken et al. 2017). A permuted dataset was created by randomly distributing the log-intensities of the gene under study over the genotypes. Then, the previous eQTL mapping model was performed on this permuted dataset. This procedure was repeated 100 times for each stage. The threshold was determined using:

$$\frac{\text{FDS}}{\text{RDS}} \leq \frac{m_0}{m} q.\log(m),$$

where, at a specific significance level, the false discoveries (FDS) were the averaged permutation result, and real discoveries (RDS) were the outcome of the eQTL mapping using the unpermuted dataset. The number of true hypotheses tested (m_0) was 29,913 - RDS, and the number of hypotheses (m) tested was the number of genes, which was 29,913. For the q-value, we used a threshold of 0.05. As a result, we got a threshold of 4.2 for PD and AR, 4.1 for IM, and 4.3 for RP.

The confidence interval of an eQTL was determined based on a -$\log_{10}(p$-value) drop of 1.5 compared to the peak marker (as in Keurentjes et al. 2007; Cubillos et al. 2012). We determine an eQTL as local if the peak marker or the confidence interval lies within 1 Mb or less from the target gene location (as in Cubillos et al. 2012). All eQTLs that did not meet this criterion were defined as distant.

We defined a region as an eQTL hotspot if the number of distant-eQTLs mapped to a particular genomic region significantly exceeded the expectation. First, we divided the genome into bins of 2 Mb. Then, we determined the expected number of distant-eQTLs per genomic bin by dividing the total number of distant-eQTLs by the total number of bins. Based on a Poisson distribution, any bin having an actual number of distant-eQTLs larger than expected ($p < 0.0001$) was then considered as an eQTL hotspot.

Gene regulatory network inference and candidate genes prioritization of eQTL hotspot

We used a community-based approach to infer regulatory networks of genes with an eQTL on a hotspot location using expression data. In this approach, we assume the hotspot is caused by a polymorphism in or near one or more regulatory genes causing altered expression that can

be detected as a local eQTL (Joosen et al. 2009; Breitling et al. 2008; Jimenez-Gomez et al. 2010; Serin et al. 2017). Based on this assumption, we labeled all genes with a local eQTL on a hotspot as candidate regulators and genes with a distant eQTL as targets. The expression of these genes was subjected to five different network inference methods to predict the interaction weight. The methods used were TIGRESS (Haury et al. 2012), Spearman correlation, CLR (Faith et al. 2007), ARACNE (Margolin et al. 2006), and GENIE3 (Huynh-Thu et al. 2010). The predictions from GENIE3 were used to establish the direction of the interaction by removing the one that has the lowest variable importance to the expression of the target genes between two pairs of genes. For instance, if the importance of $gene_i – gene_j$ is smaller than $gene_j – gene_i$, then the former is removed. By averaging the rank, the predictions of all inference methods were integrated to produce a robust and high performance prediction (Marbach et al. 2012). The threshold was determined as the minimum average rank where all nodes are included in the network. Finally, the network was visualized using Cytoscape (version 3.7.1) (Shannon et al. 2003), and network properties were calculated using the NetworkAnalyzer tool (Assenov et al. 2008). The candidate genes for each eQTL hotspot were prioritized based on their outdegree and closeness centrality (Pavlopoulos et al. 2011).

Data availability

The list of genetic markers, genotype, and gene expression data used in this study are given in Table S7, Table S8, and Table S9, respectively. Cel files of microarray data have been deposited in the ArrayExpress database at EMBL-EBI (www.ebi.ac.uk/arrayexpress) under accession number E-MTAB-9080. The phenotype and metabolite measurement can be found in Table S10 and Table S11. The list of differentially expressed genes is in Table S12. All QTL mapping results are given in Table S13 (expression QTL), Table S14 (phenotype QTL), and Table S15 (metabolite QTL). The code for the analysis and visualization is available in

269   the form of R scripts at the Wageningen University GitLab repository

270   (https://git.wur.nl/harta003/seed-germination-qtl).

271

272

273   **RESULTS**

274   **Major transcriptional shifts take place after water imbibition and radicle protrusion**

275   To visualize the transcriptional states of the parental lines and the RILs at the four seed

276   germination stages, we performed a principal component analysis using the log-intensities of

277   all expressed genes (Figure 1). The first principal component explains 55.6% of the variation

278   and separates the samples into three groups. Germination progresses from left to right with the

279   PD and AR seeds grouping together, indicating that the after-ripening treatment does not

280   induce a considerable change in global transcript abundance. The large-scale transcriptome

281   change only happens after water imbibition and radicle protrusion. This event was also

282   observed by Finch-Savage et al. (2007) and Silva et al. (2016). The second principal

283   component on the PCA explains 14.2% variance in the data and separates the RILs within

284   each of the three clusters but not the parents. The source of this variation may be the genetic

285   variation among samples and shows transgressive segregation of gene expression in RILs due

286   to genetic reshuffling of the parental genomes during crossing and generations of selfing.

287   To identify specific expression patterns among genes in the course of seed germination, we

288   performed an additional analysis of the transcriptome data using hierarchical clustering

289   (Figure 2). For this analysis, we only selected the 990 genes with a minimal fold change of

290   two between any two consecutive stages (PD to AR, AR to IM, IM to RP). We then clustered

291   both the genes and the seed samples. As shown in the figure, the clustering of samples shows

similar grouping as in the previous PCA plot; three clusters were formed with one cluster

containing both PD and AR, while IM and RP form separate clusters.

The clustering of genes shows at least three distinctive gene expression patterns. In the first

pattern, transcript abundance is highest in the last stage, radicle protrusion. A GO enrichment

test suggests that transcripts with this expression pattern are involved in the transition from

the heterotrophic seed to the autotrophic seedling stage, with enriched processes such as

photosynthesis, response to various light, and response to temperature. This is in agreement

with Rajjou et al. (2004), who showed that genes required for seedling growth are expressed

after water imbibition. The second pattern shows an opposite trend with higher transcript

abundances in the first three stages and lower expression at the end of the seed germination

process. Some of these transcripts may be the remnant of seed development since the GO

term related to this process is overrepresented. Moreover, transcripts involved in response to

hydrogen peroxide were also overrepresented, which provides more evidence for the

importance of reactive oxygen species in seed germination (for review see Wojtyla et al.

2016). The last pattern represents genes that are upregulated at the IM stage. Genes with this

pattern are functionally enriched in the catabolism of fatty acids, a likely source of energy for

seedling growth (Bewley et al. 2013c). Altogether, these results suggest that co-expression

patterns of genes reflect particular functions during the seed germination process.

Distant eQTLs explain less variance than local eQTLs and are more specific to a seed germination stage

To map loci associated with gene expression levels, we performed eQTL mapping of 29,913

genes for each seed population representing four seed germination stages (Table 1). We found

eQTLs, numbers ranging from 1,335 to 1,719 per stage (FDR = 0.05), spread across the

genome. Among the genes with an eQTL, only a few (less than 1%) had more than one. We then categorized the eQTLs into local and distant based on the distance between the target gene and the eQTL peak marker or the confidence interval. Based on this criterion, over 72% of the eQTLs per stage were categorized as local (located within 1 Mb of the gene), while the remainder were distant. Although the total of the identified eQTLs was different between the stages, the ratio of distant to local eQTLs was relatively similar for all stages. We then calculated the fraction of the total variation that is explained by the simple linear regression model for each eQTL. By comparing the density distributions (Figure S1), we showed that local eQTLs generally explain a more substantial fraction of gene expression variation than distant eQTLs. Finally, we determined the number of specific and shared eQTLs across stages (Figure 3). Here, we show that distant eQTLs are more specific to seed germination stages. Local eQTLs, on the other hand, are commonly shared between two or more stages, which is in line with previous experiments showing overlapping local eQTLs and specific distant eQTLs across different developmental stages (Vinuela et al. 2010), environments (Snoek et al. 2012; Snoek et al. 2017; Lowry et al. 2013) and populations (Cubillos et al. 2012).

An eQTL hotspot on chromosome 5 is associated with genes related to seed germination and collocates with multiple metabolic and phenotypic QTLs

To get an overview of how the eQTLs were mapped over the genome, we visualized the eQTL locations and their associated genes on a local/distant eQTL plot (Figure 4A). Here, the local eQTLs are aligned across the diagonal and spread relatively equally across the genome, while it is not the case for the distant eQTLs. Furthermore, specific loci show clustering of eQTLs, which could indicate the presence of major regulatory genes that cause genome-wide gene expression changes. We identified ten so-called (distant-) eQTL hotspots, with at least two hotspots per stage (Table 2). The number of distant eQTLs located within these hotspots

341 ranges from 16 to 96. The major eQTL hotspots are PD2, IM2, and RP4, with 69, 69, and 96

342 distant eQTLs co-locating, respectively. Moreover, the landscape of the eQTL hotspots

343 (Figure 4B) differs for every stage, including PD and AR, which is surprising since these two

344 stages have a relatively similar transcriptome profile (Figure 1).

345 We remapped the QTLs for previously studied seed germination phenotypes (Joosen et al.

346 2012) and metabolites (Joosen et al. 2013) using the RNA-seq based genetic map (Serin et al.

347 2017). We then visualized the resulting QTL count histograms alongside the eQTL histogram

348 (Figure 5). The histogram shows that several eQTL hotspots collocate with hotspots for

349 phenotype and metabolite QTLs (phQTLs and mQTLs, respectively). The most striking

350 example is the collocation of QTLs on chromosome 5 around 24—25 Mb (IM2 and RP4) at

351 the last two stages of seed germination. We performed gene ontology (GO) term enrichment

352 analysis for genes with an eQTL mapping to these hotspots, and found 'seed germination'

353 enriched among other terms (Table 2). These findings taken together indicate that the IM2 and

354 RP4 hotspots harbor one or more important genes affecting gene expression during seed

355 germination. Therefore, the identification of the regulatory gene(s) for one of these hotspots

356 can give us more insight into the trans-regulation of gene expression during seed germination.

357

358 **Transcription factors were prioritized as the candidate genes for major eQTL hotspots**

359 To prioritize the candidate regulatory genes underlying eQTL hotspots in this study, we

360 constructed a network based on the expression of genes with eQTLs on the hotspot location.

361 We built the network for two hotspots: RP4, where QTLs for expression, metabolite, and

362 phenotype are collocated; and PD2, another major eQTL hotspot in this study. For RP4, the

363 total number of genes used to construct the network was 116, of which 20 had a local eQTL at

364 the hotspot, whereas for PD2, 114 genes were identified, of which 45 with a local eQTL. The

365 genes with local eQTLs were then labeled as candidates. The networks were constructed by

integrating predictions from several gene regulatory network inference methods to ensure the robustness of the result (Marbach et al. 2012). The direction of the edges in the network is predicted using the GENIE3 method (Huynh-Thu et al. 2010). For each candidate gene, we calculated the outdegree, indicating the number of outgoing edges of a gene to other genes in the network, and the closeness centrality of the candidate gene nodes, which shows the efficiency of the gene in spreading information to the rest of the genes in the network (Pavlopoulos et al. 2011). Finally, these two network properties were used to prioritize the most likely regulator of the distant eQTL hotspot.

In the resulting network, genes encoding the transcription factors DECREASE WAX BIOSYNTHESIS/DEWAX (AT5G61590), and INDUCER OF CBP EXPRESSION 1/ICE1 (AT3G26744) were prioritized as the most likely candidate genes for RP4 (Figure 6) and PD2 (Figure 7), respectively. As many as 15 genes were predicted to be associated with DEWAX and 32 genes with ICE1. Note that these numbers depend on the chosen threshold; nonetheless, the current candidates are robust to changes when the parameter was changed (Table S3 and Table S4). Furthermore, these two genes also had the highest closeness centrality among the other candidates, showing that these genes have a strong influence within the network. We assessed the Bay x Sha SNP data (Genomes Consortium. Electronic address and Genomes 2016) and found several SNPs between the Bay and Sha parents in both the DEWAX and ICE1 genes, including two that affect the amino acid sequence of the corresponding proteins (Table S5 and Table S6). Also, querying for DEWAX and ICE1 on AraQTL showed a local eQTL for both genes in an experiment using the same RIL population on leaf tissue (West et al. 2007). This evidence supports the hypothesis that polymorphisms between the Bay and Sha alleles of DEWAX and ICE1 are be responsible for the steadily occurring local eQTLs at three stages (PD, IM, RP) for DEWAX and all four stages for ICE1.

DISCUSSION

The function of DEWAX may be related to seed cuticular wax biosynthesis

393 In this study, we constructed a network of genes associated with the RP4 eQTL hotspot and

394 showed that *DEWAX* was prioritized as the candidate gene for the hotspot. *DEWAX* encodes

395 an AP2/ERF-type transcription factor that is well-known as a negative regulator of cuticular

396 wax biosynthesis (Go et al., 2014; Suh and Go, 2014; Cui et al., 2016; Li et al., 2019) and a

397 positive regulator of defense response against biotic stress (Froschel et al. 2019; Ju et al.

398 2017). This gene also seems to be involved in drought stress response (Huang et al. 2008) by

399 inducing the expression of genes that confer drought tolerance (Sun et al. 2016), some of

400 which (*LEA4-5*, *LTI-78*) have a distant eQTL at the RP4 hotspot. Moreover, the

401 overexpression of *DEWAX* in Arabidopsis increases the seed germination rate (Sun et al.

402 2016). The role of *DEWAX* in seed germination is still unknown but may be related to

403 cuticular wax biosynthesis.

404 Wax is a mixture of hydrophobic lipids, which is part of the plant cuticle together with cutin

405 and suberin (Yeats and Rose 2013). Previous studies have demonstrated that the biosynthesis

406 of wax in the cuticular layer of stems and leaves is negatively regulated by *DEWAX* (Go et al.,

407 2014; Suh and Go, 2014; Cui et al., 2016; Li et al., 2019). Although the function of this gene

408 has never been reported in seeds, the presence of a cuticular layer indeed plays a significant

409 role in maintaining seed dormancy (Nonogaki 2019; De Giorgi et al. 2015). In Arabidopsis

410 seeds, the thick cuticular structure covering the endosperm prevents cell expansion and testa

411 rupture that precede radicle protrusion. Besides, this layer also reduces the diffusion of

412 oxygen into the seed, thus preventing oxidative stress that may cause rapid seed aging and

413 loss of dormancy (De Giorgi et al. 2015).

Besides *DEWAX*, *MUM2* is another possible regulatory gene for the RP4 hotspot based on QTL confirmation of an imbibed seed size phenotype using a heterogeneous inbred family approach (Joosen et al. 2012). In our study, we also discovered that most eQTLs on the RP4 hotspot peak at the marker located closely to the MUM2 location (Figure S2), which provides more evidence for this gene as the regulator for the hotspot. *MUM2* encodes a cell-wall modifying beta-galactosidase involved in seed coat mucilage biosynthesis, and the *mum2* mutant is characterized by a failure in extruding mucilage after water imbibition (Dean et al. 2007). In our analysis, *MUM2* did not have a distant eQTL on the RP4 hotspot; thus, it is not prioritized as a prominent candidate, pointing out a limitation of our approach in prioritizing candidate eQTL hotspot genes which will be discussed later. Nonetheless, we found some evidence connecting *DEWAX* to *MUM2*. First, Shi et al. (2019) found out that the mutant of *CPL2*, another gene involved in wax biosynthesis, showed a delayed secretion of the enzyme encoded by *MUM2* that disrupts seed coat mucilage extrusion. In the same study, they revealed that *CPL2* encodes a phosphatase involved in secretory protein trafficking required for the secretion of extracellular matrix materials, including wax and the cell wall-modifying enzyme MUM2. Although no direct connection between DEWAX and CPL2 has been reported, a recent study by Xu et al. did identify *DEWAX* as a putative regulator of cell-wall-loosening *EXPANSIN* (*EXPA*) genes involved in germination (Xu et al. 2020). These findings provide a link between wax biosynthesis and cell-wall modifying enzymes, and possibly between the genes involved in these processes.

Second, the expression of *DEWAX* may be the consequence of the disruption of seed mucilage extrusion. Penfield et al. (2001) suggest that seed mucilage helps enhance water uptake to ensure efficient germination in the condition of low water potential. This is supported by the evidence that the mucilage-impaired mutant showed reduced maximum germination only on osmotic polyethylene glycol solutions (Penfield et al. 2001). Therefore, the absence of

439   mucilage in imbibed seed under low water potential may cause osmotic stress in the seed and,

440   in turn, induce the expression of DEWAX, which is known to play a role in the response of

441   plants against osmotic stress (Sun et al. 2016). If this is the case, then a scenario could be that

442   DEWAX acts downstream of MUM2, and the expression variation of these two genes lead to

443   the emergence of the RP4 eQTL hotspot.

444

Network analysis shows the involvement of ICE1 as a regulator of gene expression

445   **during seed germination**

446

447   ICE1 is an MYC-like basic helix-loop-helix (bHLH) transcription factor that shows

448   pleiotropic effects in plants. Earlier studies of ICE1 mostly focus on the protein function in

449   the acquisition of cold tolerance (Lee et al. 2005; Chinnusamy et al. 2003) and stomatal

450   lineage development (Kanaoka et al. 2008). Recently, ICE1 was also shown to form a

451   heterodimer with ZOU, another bHLH transcription factor, to regulate endosperm breakdown

452   required for embryo growth during seed development (Denay et al. 2014). At a later stage,

453   ICE1 negatively regulates ABA-dependent pathways to promote seed germination and

454   seedling establishment (Liang and Yang 2015). This process involves repressing the

455   expression of transcription factors in ABA signaling, such as ABI3 and ABI5, and ABA-

456   responsive genes, such as *EM6* and *EM1*, thus initiating seed germination and subsequent

457   seedling establishment (Hu et al. 2019; MacGregor et al. 2019). Loss of *ice1* has been

458   reported to lead to reduced germination (MacGregor et al., 2019)

459   In this study, we performed a network analysis for genes having distant eQTLs on the PD2

460   hotspot and prioritized ICE1 as the most likely regulator using network analysis. The high

461   connectivity of ICE1 with the other genes in the network could reflect an essential regulatory

462   function of this gene during seed germination. However, we did not find any of the known

463   ICE1 target genes (i.e., *ABI3*, *ABI5*, *EM1*, and *EM6*) nor seed germination phenotype (Figure

464   5) having an eQTL at the *ICE1* locus. It could be that the ICE1 polymorphism is not severe

465   enough to cause considerable trait variation, especially to break a robust biological system

466   where several buffering mechanisms exist to prevent small molecular perturbation from

467   propagating to the phenotypic level (Signor and Nuzhdin 2018; Fu et al. 2009).

468   A good strategy to validate that a predicted candidate gene indeed causes a QTL hotspot

469   would be to test one parent's allele of the gene in the genetic background of the other parent.

470   This could be achieved by generating near-isogeneic lines, although rapid developments in

471   site directed mutagenesis might offer a more feasible high-throughput approach for future

472   studies. Next, being able to convert one parent's gene into the other parent's gene one SNP at

473   a time would even allow identification of causal SNPs.

474   **Limitations of co-expression network in identifying candidate genes of eQTL hotspots**

475   The construction of a co-expression network is a promising approach to prioritize candidate

476   eQTL genes (Serin et al. 2016). Despite its potential, there is a major limitation in using a co-

477   expression network. The network is based on gene expression data; hence the identified

478   causal genes are those that directly affect gene expression. For example, as we described

479   above, our approach did not prioritize *MUM2* for the RP4 hotspot, possibly because the gene

480   does not cause variation in the target gene expression but rather causes differences at another

481   level of target gene regulation (e.g., enzyme biosynthesis) between two parental alleles in the

482   RIL population. Other studies reported similar results where a known causal gene was not

483   detected as a hub in the network (Jimenez-Gomez et al. 2010; Sterken et al. 2017). To

484   overcome this, future work should focus on networks that are built upon multi-omics data by

485   including metabolic, proteomic, and, more importantly, phenotypic measurement data (Hawe

486   et al. 2019). Moreover, prior biological knowledge, including protein-protein interaction

487   (Szklarczyk et al. 2017), transcription factor binding-site (Kulkarni et al. 2018), and other

types of interactions (for review see Kulkarni and Vandepoele 2019) can be incorporated to

construct data-driven interaction networks. Nevertheless, our approach offers a simple and

straightforward way to prioritize candidate genes underlying eQTL hotspots from a limited

amount of resources.

Tables

Table 1. Summary of the eQTL mapping for the four different seed germination stages

stage	eQTLs	genes with an eQTL	eQTL type	total	proportion
primary dormant	1,335	1,328	local	955	0.72
			distant	380	0.28
after-ripened	1,395	1,377	local	1,089	0.78
			distant	306	0.22
six hours after imbibition	1,719	1,702	local	1,320	0.77
			distant	399	0.23
radicle protrusion	1,426	1,418	local	1,096	0.77
			distant	330	0.23

Table 2. Distant eQTL hotspots of the four seed germination stages. These hotspots were identified by dividing the genome into bins of 2 Mbp and performing a test to determine whether the number of distant eQTLs on a particular bin is higher than expected ($p > 0.0001$) assuming a Poisson distribution. Seed germination phenotype and metabolite data were taken from Joosen et al. (2012) and Joosen et al. (2013), respectively. Detailed information about enriched GO terms, metabolite, and phenotype can be seen on Supplemental Table S2 in the Supplementary Material.

hotspot ID	position	distant eQTLs	enriched GO terms	metabolite QTL	phenotype QTL
PD1	ch1:6-10 Mb	43	11	1	4
PD2	ch3:8-12 Mb	69	3	2	1
AR1	ch2:12-14 Mb	16	0	0	0
AR2	ch3:2-4 Mb	20	9	1	1

IM1	ch5:6-8 Mb	19	2	24	1
IM2	ch5:22-26 Mb	69	6	6	31
RP1	ch1:0-2 Mb	23	1	0	1
RP2	ch1:6-8 Mb	18	0	0	3
RP3	ch5:14-16 Mb	21	29	0	1
RP4	ch5:24-26Mb	96	18	20	25

512

513

Literature cited

Alexa, A., J. Rahnenführer, and T. Lengauer, 2006 Improved scoring of functional groups from gene expression data by decorrelating GO graph structure. *Bioinformatics* 22 (13):1600-1607.

Assenov, Y., F. Ramirez, S.E. Schelhorn, T. Lengauer, and M. Albrecht, 2008 Computing topological parameters of biological networks. *Bioinformatics* 24 (2):282-284.

Bassel, G.W., H. Lan, E. Glaab, D.J. Gibbs, T. Gerjets *et al.*, 2011 Genome-wide network model capturing seed germination reveals coordinated regulation of plant cellular phase transitions. *Proc Natl Acad Sci U S A* 108 (23):9709-9714.

Bewley, J.D., K.J. Bradford, H.W.M. Hilhorst, and H. Nonogaki, 2013a Dormancy and the Control of Germination, pp. 247-297 in *Seeds: Physiology of Development, Germination and Dormancy, 3rd Edition*, edited by J.D. Bewley, K.J. Bradford, H.W.M. Hilhorst and H. Nonogaki. Springer New York, New York, NY.

Bewley, J.D., K.J. Bradford, H.W.M. Hilhorst, and H. Nonogaki, 2013b Germination, pp. 133-181 in *Seeds: Physiology of Development, Germination and Dormancy, 3rd Edition*, edited by J.D. Bewley, K.J. Bradford, H.W.M. Hilhorst and H. Nonogaki. Springer New York, New York, NY.

Bewley, J.D., K.J. Bradford, H.W.M. Hilhorst, and H. Nonogaki, 2013c Synthesis of Storage Reserves, pp. 85-131 in *Seeds: Physiology of Development, Germination and*

Dormancy, 3rd Edition, edited by J.D. Bewley, K.J. Bradford, H.W.M. Hilhorst and H. Nonogaki. Springer New York, New York, NY.

Breitling, R., Y. Li, B.M. Tesson, J. Fu, C. Wu *et al.*, 2008 Genetical genomics: spotlight on QTL hotspots. *PLoS Genet* 4 (10):e1000232.

Brem, R.B., G. Yvert, R. Clinton, and L. Kruglyak, 2002 Genetic dissection of transcriptional regulation in budding yeast. *Science* 296 (5568):752-755.

Buijs, G., A. Vogelzang, H. Nijveen, and L. Bentsink, 2019 Dormancy cycling: Translation related transcripts are the main difference between dormant and non-dormant seeds in the field. *Plant J*.

Cadman, C.S., P.E. Toorop, H.W. Hilhorst, and W.E. Finch-Savage, 2006 Gene expression profiles of Arabidopsis Cvi seeds during dormancy cycling indicate a common underlying dormancy control mechanism. *Plant J* 46 (5):805-822.

Chinnusamy, V., M. Ohta, S. Kanrar, B.H. Lee, X. Hong *et al.*, 2003 ICE1: a regulator of cold-induced transcriptome and freezing tolerance in Arabidopsis. *Genes Dev* 17 (8):1043-1054.

Comai, L., and J.J. Harada, 1990 Transcriptional activities in dry seed nuclei indicate the timing of the transition from embryogeny to germination. *Proc Natl Acad Sci U S A* 87 (7):2671-2674.

Cubillos, F.A., J. Yansouni, H. Khalili, S. Balzergue, S. Elftieh *et al.*, 2012 Expression variation in connected recombinant populations of Arabidopsis thaliana highlights distinct transcriptome architectures. *BMC Genomics* 13:117.

De Giorgi, J., U. Piskurewicz, S. Loubery, A. Utz-Pugin, C. Bailly *et al.*, 2015 An Endosperm-Associated Cuticle Is Required for Arabidopsis Seed Viability, Dormancy and Early Control of Germination. *PLoS Genet* 11 (12):e1005708.

557 Dean, G.H., H. Zheng, J. Tewari, J. Huang, D.S. Young *et al.*, 2007 The Arabidopsis MUM2
558   gene encodes a beta-galactosidase required for the production of seed coat mucilage
559   with correct hydration properties. *Plant Cell* 19 (12):4007-4021.

560 Dekkers, B.J., S. Pearce, R.P. van Bolderen-Veldkamp, A. Marshall, P. Widera *et al.*, 2013
561   Transcriptional dynamics of two seed compartments with opposing roles in
562   Arabidopsis seed germination. *Plant Physiol* 163 (1):205-215.

563 Denay, G., A. Creff, S. Moussu, P. Wagnon, J. Thevenin *et al.*, 2014 Endosperm breakdown
564   in Arabidopsis requires heterodimers of the basic helix-loop-helix proteins ZHOUPI
565   and INDUCER OF CBP EXPRESSION 1. *Development* 141 (6):1222-1227.

566 Faith, J.J., B. Hayete, J.T. Thaden, I. Mogno, J. Wierzbowski *et al.*, 2007 Large-scale
567   mapping and validation of Escherichia coli transcriptional regulation from a
568   compendium of expression profiles. *PLoS Biol* 5 (1):e8.

569 Finch-Savage, W.E., C.S. Cadman, P.E. Toorop, J.R. Lynn, and H.W. Hilhorst, 2007 Seed
570   dormancy release in Arabidopsis Cvi by dry after-ripening, low temperature, nitrate
571   and light shows common quantitative patterns of gene expression directed by
572   environmentally specific sensing. *Plant J* 51 (1):60-78.

573 Froschel, C., T. Iven, E. Walper, V. Bachmann, C. Weiste *et al.*, 2019 A Gain-of-Function
574   Screen Reveals Redundant ERF Transcription Factors Providing Opportunities for
575   Resistance Breeding Toward the Vascular Fungal Pathogen Verticillium longisporum.
576   *Mol Plant Microbe Interact* 32 (9):1095-1109.

577 Fu, J., J.J. Keurentjes, H. Bouwmeester, T. America, F.W. Verstappen *et al.*, 2009 System-
578   wide molecular evidence for phenotypic buffering in Arabidopsis. *Nat Genet* 41
579   (2):166-167.

580   Genomes Consortium. Electronic address, m.n.g.o.a.a., and C. Genomes, 2016 1,135

581   Genomes Reveal the Global Pattern of Polymorphism in Arabidopsis thaliana. *Cell*

582   166 (2):481-491.

583   Haury, A.C., F. Mordelet, P. Vera-Licona, and J.P. Vert, 2012 TIGRESS: Trustful Inference

584   of Gene REgulation using Stability Selection. *BMC Syst Biol* 6:145.

585   Hawe, J.S., F.J. Theis, and M. Heinig, 2019 Inferring Interaction Networks From Multi-

586   Omics Data. *Front Genet* 10:535.

587   Hu, Y., X. Han, M. Yang, M. Zhang, J. Pan *et al.*, 2019 The Transcription Factor INDUCER

588   OF CBF EXPRESSION1 Interacts with ABSCISIC ACID INSENSITIVE5 and

589   DELLA Proteins to Fine-Tune Abscisic Acid Signaling during Seed Germination in

590   Arabidopsis. *Plant Cell* 31 (7):1520-1538.

591   Huang, D., W. Wu, S.R. Abrams, and A.J. Cutler, 2008 The relationship of drought-related

592   gene expression in Arabidopsis thaliana to hormonal and environmental factors. *J Exp*

593   *Bot* 59 (11):2991-3007.

594   Huynh-Thu, V.A., A. Irrthum, L. Wehenkel, and P. Geurts, 2010 Inferring regulatory

595   networks from expression data using tree-based methods. *PLoS One* 5 (9).

596   Jansen, R., and J. Nap, 2001 Genetical genomics: the added value from segregation. *Trends in*

597   *Genetics* 17 (7):388-391.

598   Jimenez-Gomez, J.M., A.D. Wallace, and J.N. Maloof, 2010 Network analysis identifies

599   ELF3 as a QTL for the shade avoidance response in Arabidopsis. *PLoS Genet* 6

600   (9):e1001100.

601   Joosen, R.V., D. Arends, Y. Li, L.A. Willems, J.J. Keurentjes *et al.*, 2013 Identifying

602   genotype-by-environment interactions in the metabolism of germinating arabidopsis

603   seeds using generalized genetical genomics. *Plant Physiol* 162 (2):553-566.

604 Joosen, R.V., D. Arends, L.A. Willems, W. Ligterink, R.C. Jansen *et al.*, 2012 Visualizing the

605 genetic landscape of Arabidopsis seed performance. *Plant Physiol* 158 (2):570-589.

606 Joosen, R.V., W. Ligterink, H.W. Hilhorst, and J.J. Keurentjes, 2009 Advances in genetical

607 genomics of plants. *Curr Genomics* 10 (8):540-549.

608 Ju, S., Y.S. Go, H.J. Choi, J.M. Park, and M.C. Suh, 2017 DEWAX Transcription Factor Is

609 Involved in Resistance to Botrytis cinerea in Arabidopsis thaliana and Camelina

610 sativa. *Front Plant Sci* 8:1210.

611 Kanaoka, M.M., L.J. Pillitteri, H. Fujii, Y. Yoshida, N.L. Bogenschutz *et al.*, 2008

612 SCREAM/ICE1 and SCREAM2 specify three cell-state transitional steps leading to

613 arabidopsis stomatal differentiation. *Plant Cell* 20 (7):1775-1785.

614 Keurentjes, J.J., J. Fu, I.R. Terpstra, J.M. Garcia, G. van den Ackerveken *et al.*, 2007

615 Regulatory network construction in Arabidopsis by using genome-wide gene

616 expression quantitative trait loci. *Proc Natl Acad Sci U S A* 104 (5):1708-1713.

617 Kulkarni, S.R., and K. Vandepoele, 2019 Inference of plant gene regulatory networks using

618 data-driven methods: A practical overview. *Biochim Biophys Acta Gene Regul*

619 *Mech*:194447.

620 Kulkarni, S.R., D. Vaneechoutte, J. Van de Velde, and K. Vandepoele, 2018 TF2Network:

621 predicting transcription factor regulators and gene regulatory networks in Arabidopsis

622 using publicly available binding site information. *Nucleic Acids Res* 46 (6):e31.

623 Lee, B.H., D.A. Henderson, and J.K. Zhu, 2005 The Arabidopsis cold-responsive

624 transcriptome and its regulation by ICE1. *Plant Cell* 17 (11):3155-3175.

625 Lelli, K.M., M. Slattery, and R.S. Mann, 2012 Disentangling the many layers of eukaryotic

626 transcriptional regulation. *Annu Rev Genet* 46:43-68.

26

Leubner-Metzger, G., 2005 beta-1,3-Glucanase gene expression in low-hydrated seeds as a mechanism for dormancy release during tobacco after-ripening. *Plant J* 41 (1):133-145.

Li, Y., M.A. Swertz, G. Vera, J. Fu, R. Breitling *et al.*, 2009 designGG: an R-package and web tool for the optimal design of genetical genomics experiments. *BMC Bioinformatics* 10 (1):188.

Liang, C.H., and C.C. Yang, 2015 Identification of ICE1 as a negative regulator of ABA-dependent pathways in seeds and seedlings of Arabidopsis. *Plant Mol Biol* 88 (4-5):459-470.

Loudet, O., S. Chaillou, C. Camilleri, D. Bouchez, and F. Daniel-Vedele, 2002 Bay-0 $\times$ Shahdara recombinant inbred line population: a powerful tool for the genetic dissection of complex traits in Arabidopsis. *Theoretical and Applied Genetics* 104 (6):1173-1184.

Lowry, D.B., T.L. Logan, L. Santuari, C.S. Hardtke, J.H. Richards *et al.*, 2013 Expression quantitative trait locus mapping across water availability environments reveals contrasting associations with genomic features in Arabidopsis. *Plant Cell* 25 (9):3266-3279.

MacGregor, D.R., N. Zhang, M. Iwasaki, M. Chen, A. Dave *et al.*, 2019 ICE1 and ZOU determine the depth of primary seed dormancy in Arabidopsis independently of their role in endosperm development. *Plant J* 98 (2):277-290.

Marbach, D., J.C. Costello, R. Kuffner, N.M. Vega, R.J. Prill *et al.*, 2012 Wisdom of crowds for robust gene network inference. *Nat Methods* 9 (8):796-804.

Margolin, A.A., I. Nemenman, K. Basso, C. Wiggins, G. Stolovitzky *et al.*, 2006 ARACNE: an algorithm for the reconstruction of gene regulatory networks in a mammalian cellular context. *BMC Bioinformatics* 7 Suppl 1:S7.

Nakabayashi, K., M. Okamoto, T. Koshiba, Y. Kamiya, and E. Nambara, 2005 Genome-wide profiling of stored mRNA in Arabidopsis thaliana seed germination: epigenetic and genetic regulation of transcription in seed. *Plant J* 41 (5):697-709.

Narsai, R., S.R. Law, C. Carrie, L. Xu, and J. Whelan, 2011 In-depth temporal transcriptome profiling reveals a crucial developmental switch with roles for RNA processing and organelle metabolism that are essential for germination in Arabidopsis. *Plant Physiol* 157 (3):1342-1362.

Nijveen, H., W. Ligterink, J.J. Keurentjes, O. Loudet, J. Long *et al.*, 2017 AraQTL - workbench and archive for systems genetics in Arabidopsis thaliana. *Plant J* 89 (6):1225-1235.

Nonogaki, H., 2019 Seed germination and dormancy: The classic story, new puzzles, and evolution. *J Integr Plant Biol* 61 (5):541-563.

Nonogaki, H., G.W. Bassel, and J.D. Bewley, 2010 Germination—Still a mystery. *Plant Science* 179 (6):574-581.

Pavlopoulos, G.A., M. Secrier, C.N. Moschopoulos, T.G. Soldatos, S. Kossida *et al.*, 2011 Using graph theory to analyze biological networks. *BioData Min* 4:10.

Penfield, S., R.C. Meissner, D.A. Shoue, N.C. Carpita, and M.W. Bevan, 2001 MYB61 Is Required for Mucilage Deposition and Extrusion in the Arabidopsis Seed Coat. *The Plant Cell* 13 (12):2777-2791.

Rajjou, L., K. Gallardo, I. Debeaujon, J. Vandekerckhove, C. Job *et al.*, 2004 The effect of alpha-amanitin on the Arabidopsis seed proteome highlights the distinct roles of stored and neosynthesized mRNAs during germination. *Plant Physiol* 134 (4):1598-1613.

Ritchie, M.E., B. Phipson, D. Wu, Y. Hu, C.W. Law *et al.*, 2015 limma powers differential expression analyses for RNA-sequencing and microarray studies. *Nucleic Acids Research* 43 (7):e47-e47.

Rockman, M.V., and L. Kruglyak, 2006 Genetics of global gene expression. *Nat Rev Genet* 7 (11):862-872.

Serin, E.A., H. Nijveen, H.W. Hilhorst, and W. Ligterink, 2016 Learning from Co-expression Networks: Possibilities and Challenges. *Front Plant Sci* 7:444.

Serin, E.A.R., L.B. Snoek, H. Nijveen, L.A.J. Willems, J.M. Jimenez-Gomez *et al.*, 2017 Construction of a High-Density Genetic Map from RNA-Seq Data for an Arabidopsis Bay-0 x Shahdara RIL Population. *Front Genet* 8:201.

Shannon, P., A. Markiel, O. Ozier, N.S. Baliga, J.T. Wang *et al.*, 2003 Cytoscape: a software environment for integrated models of biomolecular interaction networks. *Genome Res* 13 (11):2498-2504.

Shi, L., G.H. Dean, H. Zheng, M.J. Meents, T.M. Haslam *et al.*, 2019 ECERIFERUM11/C-TERMINAL DOMAIN PHOSPHATASE-LIKE2 Affects Secretory Trafficking. *Plant Physiol* 181 (3):901-915.

Signor, S.A., and S.V. Nuzhdin, 2018 The Evolution of Gene Expression in cis and trans. *Trends Genet* 34 (7):532-544.

Silva, A.T., P.A. Ribone, R.L. Chan, W. Ligterink, and H.W. Hilhorst, 2016 A Predictive Coexpression Network Identifies Novel Genes Controlling the Seed-to-Seedling Phase Transition in Arabidopsis thaliana. *Plant Physiol* 170 (4):2218-2231.

Snoek, B.L., M.G. Sterken, R.P.J. Bevers, R.J.M. Volkers, A. Van't Hof *et al.*, 2017 Contribution of trans regulatory eQTL to cryptic genetic variation in C. elegans. *BMC Genomics* 18 (1):500.

Snoek, L.B., I.R. Terpstra, R. Dekter, G. Van den Ackerveken, and A.J. Peeters, 2012 Genetical Genomics Reveals Large Scale Genotype-By-Environment Interactions in Arabidopsis thaliana. *Front Genet* 3:317.

701 Sterken, M.G., L. van Bemmelen van der Plaat, J.A.G. Riksen, M. Rodriguez, T. Schmid *et*

702 *al.*, 2017 Ras/MAPK Modifier Loci Revealed by eQTL in Caenorhabditis elegans. *G3*

703 *(Bethesda)* 7 (9):3185-3193.

704 Sun, Z.M., M.L. Zhou, W. Dan, Y.X. Tang, M. Lin *et al.*, 2016 Overexpression of the Lotus

705 corniculatus Soloist Gene LcAP2/ERF107 Enhances Tolerance to Salt Stress. *Protein*

706 *Pept Lett* 23 (5):442-449.

707 Szklarczyk, D., J.H. Morris, H. Cook, M. Kuhn, S. Wyder *et al.*, 2017 The STRING database

708 in 2017: quality-controlled protein-protein association networks, made broadly

709 accessible. *Nucleic Acids Res* 45 (D1):D362-D368.

710 Terpstra, I.R., L.B. Snoek, J.J. Keurentjes, A.J. Peeters, and G. van den Ackerveken, 2010

711 Regulatory network identification by genetical genomics: signaling downstream of the

712 Arabidopsis receptor-like kinase ERECTA. *Plant Physiol* 154 (3):1067-1078.

713 Uygun, S., C. Peng, M.D. Lehti-Shiu, R.L. Last, and S.H. Shiu, 2016 Utility and Limitations

714 of Using Gene Expression Data to Identify Functional Associations. *PLoS Comput*

715 *Biol* 12 (12):e1005244.

716 Valba, O.V., S.K. Nechaev, M.G. Sterken, L.B. Snoek, J.E. Kammenga *et al.*, 2015 On

717 predicting regulatory genes by analysis of functional networks in C. elegans. *BioData*

718 *Min* 8:33.

719 Vinuela, A., L.B. Snoek, J.A. Riksen, and J.E. Kammenga, 2010 Genome-wide gene

720 expression regulation as a function of genotype and age in C. elegans. *Genome Res* 20

721 (7):929-937.

722 Wan, C.Y., and T.A. Wilkins, 1994 A Modified Hot Borate Method Significantly Enhances

723 the Yield of High-Quality RNA from Cotton (Gossypium hirsutum L.). *Analytical*

724 *Biochemistry* 223 (1):7-12.

725   West, M.A., K. Kim, D.J. Kliebenstein, H. van Leeuwen, R.W. Michelmore *et al.*, 2007

726   Global eQTL mapping reveals the complex genetic architecture of transcript-level

727   variation in Arabidopsis. *Genetics* 175 (3):1441-1450.

728   Wojtyla, L., K. Lechowska, S. Kubala, and M. Garnczarska, 2016 Different Modes of

729   Hydrogen Peroxide Action During Seed Germination. *Front Plant Sci* 7:66.

730   Xu, H., O. Lantzouni, T. Bruggink, R. Benjamins, F. Lanfermeijer *et al.*, 2020 A Molecular

731   Signal Integration Network Underpinning Arabidopsis Seed Germination. *Curr Biol*.

732   Yeats, T.H., and J.K. Rose, 2013 The formation and function of plant cuticles. *Plant Physiol*
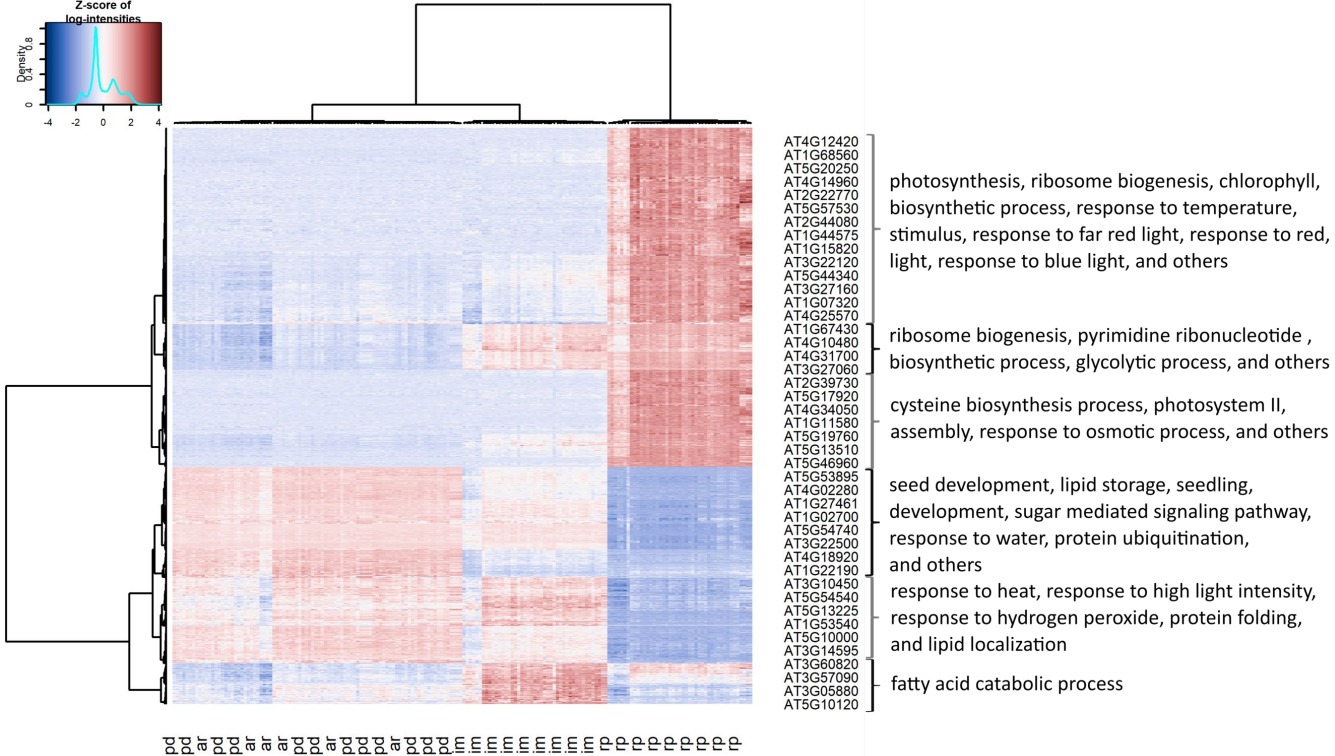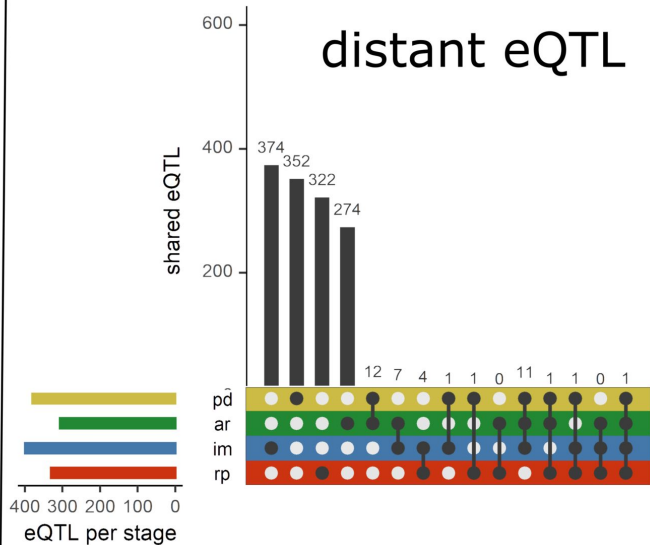
733   163 (1):5-20.

734

735

736

737
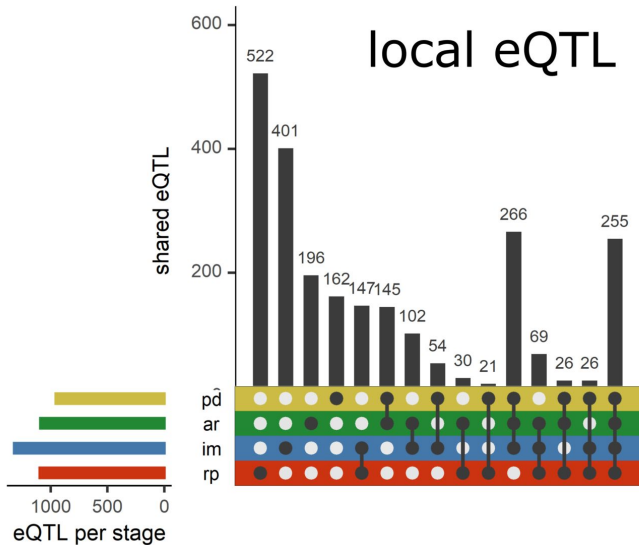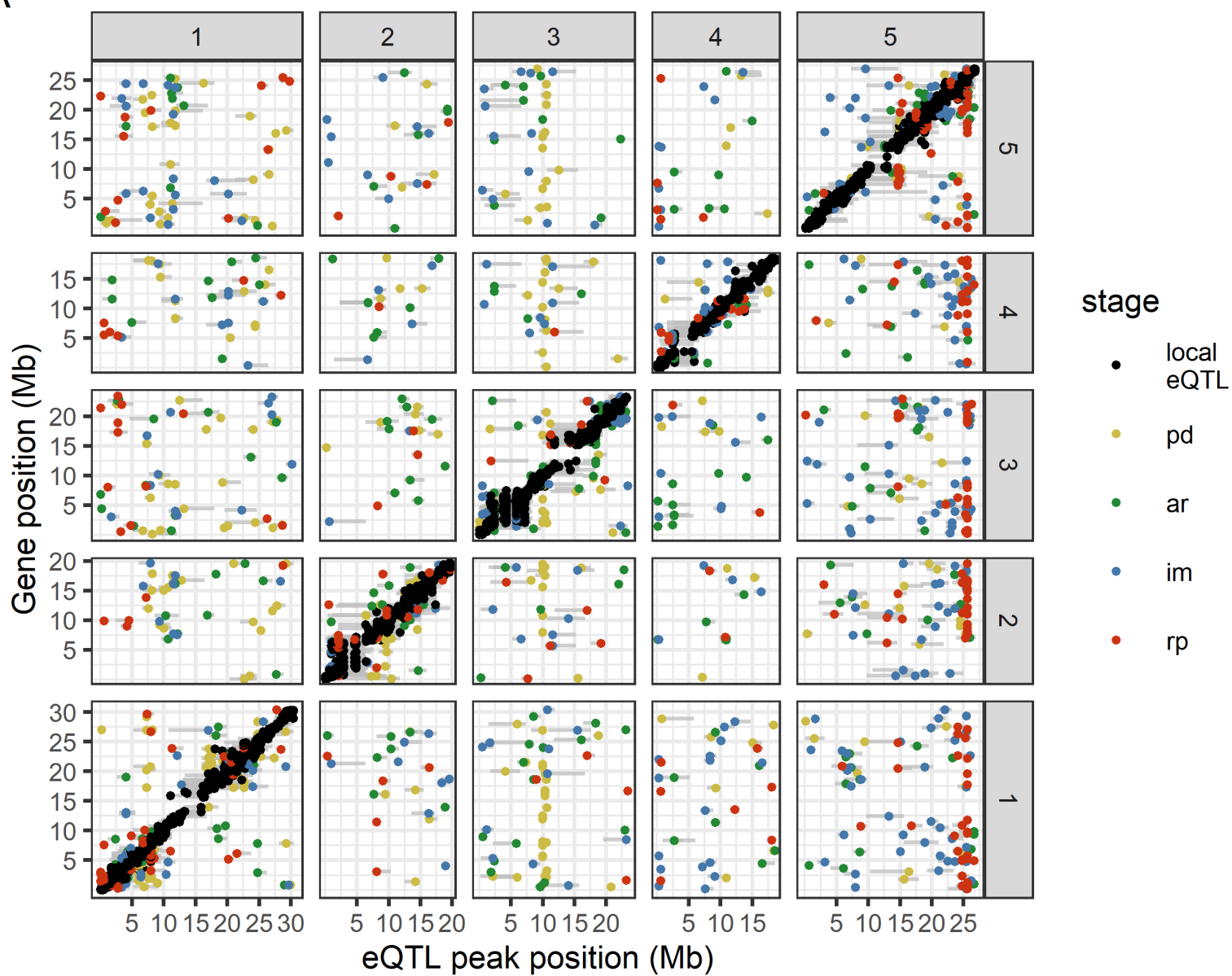
photosynthesis, ribosome biogenesis, chlorophyll, biosynthetic process, response to temperature, stimulus, response to far red light, response to red, light, response to blue light, and others

ribosome biogenesis, pyrimidine ribonucleotide, biosynthetic process, glycolytic process, and others

cysteine biosynthesis process, photosystem II, assembly, response to osmotic process, and others

seed development, lipid storage, seedling, development, sugar mediated signaling pathway, response to water, protein ubiquitination, and others

response to heat, response to high light intensity, response to hydrogen peroxide, protein folding, and lipid localization

fatty acid catabolic process

gene	Out-degree	Closeness Centrality	description
AT5G61590/DEWAX	15	0.45	transcription factor in cutin biosynthesis
AT5G62490/HVA22B	14	0.44	ABA-responsive protein
AT5G62540/UBC3	10	0.41	ubiquitin conjugating enzyme
AT5G59690	7	0.24	histone superfamily protein
AT5G63020/SUT1	7	0.27	NB-LRR mediating immune response
AT5G63030/GRXC1	6	0.25	Thioredoxin superfamily protein
AT5G63150	4	0.23	hypothetical protein
AT5G64510/TIN1	3	0.23	ER stress-inducible protein
AT5G65060/MAF3	3	0.23	MADS-box transcription factor family protein
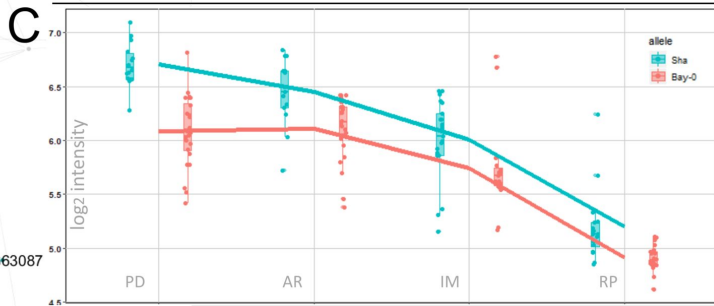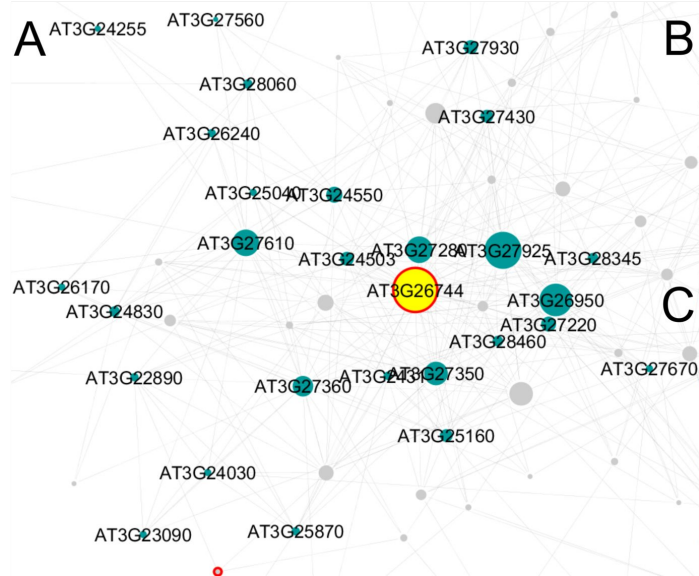
gene	Out-degree	Closeness Centrality	description
AT3G26744/ICE1	32	0.54	MYC-like bHLH transcriptional activator
AT3G27925/DEG1	27	0.51	DegP protease
AT3G26950	26	0.46	unknown protein
AT3G27280/PHB4	20	0.46	Prohibitin-4
AT3G27610	18	0.42	Nucleotidylyl transferase superfamily protein
AT3G27350	16	0.44	Transcriptional regulator ATRX -like protein
AT3G27360/H3.1	16	0.43	Histone superfamily protein
AT3G24550	13	0.40	Heavy metal transport superfamily protein
AT3G27220/ARI4	9	0.37	IBR domain containing protein
AT3G24503/ALDH1A	8	0.34	Aldehyde dehydrogenase